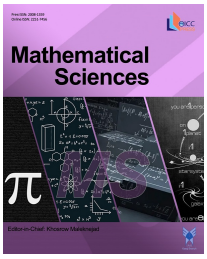

Math. Sci. 2026; 20(1): 30-47

Mathematical Sciences (MS)

https://doi.org/10.57647/mathsci.2026.2001.02

Research Article

Photo-electro-magneto-thermoelastic Excitation Rotating Semiconductor Medium based on Focused Laser Beam

Kawther K. Alarfaj[1], Ahamd .F. Al-Hazaemh[2,*], Abdel M. Abd-Alla[2], Salah E. Abbas[2],

[1]*Department of Mathematics and Statistics, College of Science, King Faisal University, P.O. Box 400, Al-Ahsa 31982, Saudi Arabia*
[2]*Mathematics Department, Faculty of Science, Sohag University, Sohag, Egypt*

[*]**Corresponding author:** Ahmadfaruk25@icloud.com

Article History

Received:
18 December 2025

Revised:
12 January 2026

Accepted:
27 January 2026

Published online:
12 February 2026

Published in Issue:
31 March 2026

Abstract:

This study aims to develop an advanced model for the propagation of photo electro-magneto-thermoelastic waves in rotating, nonlocal semiconductor media subjected to pulsed laser beam. The novelty of this work lies in formulating a new coupled dynamic model that integrates photothermal, mechanical stresses and carrier density with temperature interactions in an elastic semiconductor medium. The resulting coupled system for temperature, displacement, stress, and plasma density is solved using the normal-mode technique under pulsed laser beam. Numerical simulations are carried out for Silicon material to explore the influence of the electro-magnetic field and rotation. Results show that lowering the rotation produces slower thermal decay and enhanced oscillations in displacement components, reflecting long-memory heat transport at the Nano scale. Electro-magnetic field significantly modifies temperature profiles and stress amplitudes, with stronger effects near the heated surface. Rotation affect wave dispersion, while the electro-magnetic field interaction governs energy absorption and stress localization. The research presents, for the first time, electro-magnetic field photo thermoacoustic formulation for rotating semiconductors with temperature-dependent conductivity. The model enriches the theoretical understanding of ultrafast laser–matter interactions, offering guidance for the design of semiconductor devices and MEMS sensors, diagnostics operating under rapid or high-intensity thermal loads. The results are represented graphically to assess the influences of the rotation and electro-magnetic field on the plasma, thermal, and elastic waves.

Keywords: Semiconductor material; Normal mode; Lame's potential; Thermoelastic waves; Focused laser beam; Generalized thermoelastic theories; Electromagnetic field; Rotation

Cite this article: Alarfaj K. K., Al-Hazaemh A. F., Abd-Alla A. M., Abbas S. E. Photo-electro-magneto-thermoelastic Excitation Rotating Semiconductor Medium based on Focused Laser Beam. Math. Sci 2026; *20*(1): 30-47 https://doi.org/10.57647/mathsci.2026.2001.02

1. Introduction

In recent years, the investigation of wave propagation and memory effects in thermoelastic media has garnered significant attention due to its vast applications in geophysics, biomechanics, aerospace engineering, and advanced material science. The traditional models of thermoelasticity, both uncoupled and coupled, are predicated on the unrealistic postulate that thermal signals propagate at an infinite velocity, a notion at odds with empirical evidence showcasing finite-speed wave propagation. In response to this discrepancy, advanced theoretical frameworks such as those introduced by Lord-Shulman (L-S) and Green and Lindsay (G-L) have been developed. These models introduce the concept of a limited heat transport velocity, leading to a revised formulation of the heat conduction equation that better aligns with experimental observations ([1, 2, 3, 4, 5]). By in-

corporating the concept of finite thermal signal velocity, these non-classical theories provide a more accurate and practical basis for the analysis of thermoelastic phenomena. Biot [1] introduced the coupled theory of thermoelasticity, where the equations of elasticity and heat conduction are coupled. Lord and Shulman [2] formulated a generalized dynamical theory of thermoelasticity using a form of the heat transport equation. Dhaliwal and Sherief [3] derived the equations of generalized thermoelasticity for an anisotropic medium. Ignaczak [4] formulated a generalized theory of linear thermoelasticity with a single relaxation time. Ignaczak [5] established a initial boundary-value problem of linear dynamic thermoelasticity with one Anwar and Sherief [6] adopted the stale space approach for the solution of coupled thermoelastic problems for the solution of one-dimensional problem in generalized thermoelasticity. Sherief [7] studied the equations of generalized thermoelasticity with one relaxation time for D1 problem including heat sources in the state space with Laplace transform techniques. Sherief and Anwar [8] discussed the state-space formulation for two-dimensional problems of generalized thermoelasticity with one relaxation time using Laplace and Fourier integral transformation. Sherief [9] examined the solution of the problem of determining stress and temperature equations of generalized thermoelasticity using the Laplace transform technique. Sherief and Hamza [10] explored the two-dimensional problem of a thick plate whose lower and upper surfaces are traction free and subjected to a given axisymmetric temperature distribution. Eringen [11] and Suhubi and Eringen [12] derived the basic field equations, boundary conditions and constitutive equations of micro-elastic solids which are affected by the micro-deformations and rotations. Eringen [13] extended micropolar elasticity to include the thermal effects. Ezzat and Awad [14] used normal mode analysis with Modified Ohm's law and Fourier's law to obtain the exact formulas of temperature, displacement, micro-rotation, stresses, couple stresses, electric field, magnetic field and current density. Singh and Boruah [15] investigated the problem of reflection of homogeneous plane waves from the free surface of a generalized magneto-thermoelastic half-space. Tiwari et al. [16] investigated the memory response on generalized thermoelastic medium in context of dual phase lag thermoelasticity with non-local effect. Othman et al. [17] investigated the effect of rotation on micropolar generalized thermoelasticity with two-temperatures using a dual-phase lag model. Abd-Alla and Al-Qahtani [18] studied the electro-magneto-thermoelastic wave propagation in a rotating anisotropic semiconductor. Lotfy [19] discussed the the elastic wave motions for a photothermal medium of a dual-phase-lag model with an internal heat source and gravitational field. Abd-Alla and Abo-Dahab [20] explained the Effect of rotation and initial stress on an infinite generalized magneto-thermoelastic diffusion body with a spherical cavity. Jangra et al. [21] displayed the wave propagation in a nonlocal microstretch saturated porothermoelastic medium under moore-gibson-thompson heat conduction model. Abd-Alla et al. [22] investigated the thermal shock behaviour on generalized thermoelastic medium under initial stress with rotation. Awwad et al. [23] investigated the photo-thermoelastic behavior of a functionally graded semiconductor medium excited by thermal laser pulses.

In recent years, researchers have extensively focused on the waves propagation in a photothermal semiconducting medium (see for example [24, 25, 26, 27, 28, 29, 30, 31, 32] and several references therein.

The present investigation introduces a comprehensive framework for analyzing photo-thermoelastic dynamics in rotating semiconductor media with electro-magnetic field under pulsed laser heating. Earlier, the properties of elastic constants in materials were supposed to vary along only one direction. It is possible that the properties may vary along two directions. Hence, the authors have attempted the problem to derive new results. A normal-mode solution is employed to derive analytical expressions, allowing systematic evaluation of the influence of rotation and electromagnetic field. The expressions are obtained for displacement components, temperature distribution, stress components and carrier density. The numerical evaluation of these field variables is carried out to analyze their variations. Furthermore, the effects of time, laser pulse time, angular frequency, magnetic field, electric permittivity and the wave number parameter on the system's response are illustrated graphically using Mathematica software. This cross-disciplinary formulation not only extends the theoretical foundations of photo thermoelasticity but also provides actionable insight for the optimisation of semiconductor devices, MEMS/NEMS sensors, laser-based diagnostics, and photoacoustic imaging systems operating under ultrafast or high-power thermal conditions.

2. Mathematical modelling and formulation

We consider a homogeneous, isotropic, electro-magneto-thermoelastic semiconducting medium with photothermal and rotation effect. This study is taken into consideration under the Green-Lindsay theory. Also, the origin of a rectangular Cartesian coordinate system (x, y, z) is taken at any point on the plane surface of a half-space, $x = 0$ for the 2D problem, the displacement vector $\overrightarrow{u} = (u, v, 0)$. The rotation axis is the axis perpendicular to the plane, and the whole body rotates with a uniform angular velocity $\overrightarrow{\Omega} = \Omega\overrightarrow{n}$. Consequently, there are two additional requirements for the elastodynamic equations: Centripetal acceleration $(\overrightarrow{\Omega} \wedge (\overrightarrow{\Omega} \wedge \overrightarrow{u}))$ caused by just time-varying motion, and Cariole's acceleration $(2\overrightarrow{\Omega} \wedge \dot{\overrightarrow{u}})$ caused by a moving reference frame.

The Maxwell equations of the electromagnetic field can be found as follows when the electro-dynamic

10.57647/mathsci.2026.2001.02

medium is linearized for slow motion:

$$\overrightarrow{j} = curl\,\overrightarrow{h} - \varepsilon_0 \frac{\partial \overrightarrow{E}}{\partial t}, \quad -\mu_e \frac{\partial \overrightarrow{h}}{\partial t} = curl\overrightarrow{E},$$
$$div\,\overrightarrow{h} = o, \quad div\overrightarrow{E} = 0,$$
$$\overrightarrow{E} = -\mu_e \left(\frac{\partial \overrightarrow{u}}{\partial t} \times \overrightarrow{H}\right), \quad \overrightarrow{h} = curl\left(\overrightarrow{u} \times \overrightarrow{H}\right). \quad (1)$$

where, ε_0 and $_e$ represent the electric permittivity and magnetic permeability, respectively. Also, $(\overrightarrow{u})$ denotes the particle velocity ($\overrightarrow{u}$&zir,is the displacement vector), and the dot notation denotes the time differentiation, the vector $\overrightarrow{J}$ represents the current density in the semiconductor medium, which may be taken in the direction of the electric field $\overrightarrow{E}$, the magnetic field intensity vector and the electric field intensity vector are denoted by $\overrightarrow{h}$ $(H = H_0 + h)$ and $\overrightarrow{E}$ respectively is expressed as follow:

$$H_x = H_z = 0, \quad H_y = H_0$$
$$\overrightarrow{E} = -\mu_e \begin{vmatrix} \overrightarrow{i} & \overrightarrow{J} & \overrightarrow{k} \\ \dot{u} & 0 & \dot{w} \\ 0 & H_0 & 0 \end{vmatrix} \quad (2)$$
$$E_x = \mu_e H_0 \dot{w}, \quad E_y = 0, \quad E_z = -\mu_e H_0 \dot{u}$$

From Eqs. (1), we can calculate the vector components of the current density in terms of the displacement component as

$$\overrightarrow{J} = \begin{vmatrix} \overrightarrow{i} & \overrightarrow{J} & \overrightarrow{k} \\ \frac{\partial}{\partial x} & \frac{\partial}{\partial y} & \frac{\partial}{\partial z} \\ 0 & H_0 & 0 \end{vmatrix} - \varepsilon_\circ\,(0,\ 0, -\mu_e H_0 \dot{u}\ ) \quad (3)$$
$$J_x = J_y = 0, \qquad J_z = \frac{\partial h}{\partial x} + \mu_e H_0 \varepsilon_0 \dot{u}$$

The Lorentz force vector takes the following form

$$\overrightarrow{F} = \mu_e(\overrightarrow{J}\,x\overrightarrow{H}). \quad (4)$$

where

$$\overrightarrow{H} = (0, H_0, 0), \qquad F_x = \frac{\partial \tau_{xx}}{\partial x}, \qquad F_z = \frac{\partial \tau_{zz}}{\partial z},$$

F_x and F_z are the components of Lorentz forces
(i) The equations of motion for a thermoelastic semiconductor material are [23]:

$$(\lambda + 2\mu)\frac{\partial^2 u}{\partial x^2} + (\lambda + \mu)\frac{\partial^2 v}{\partial x \partial y} + \mu \frac{\partial^2 u}{\partial y^2} - \gamma_n \frac{\partial N}{\partial x}$$
$$-\gamma_t \left(1 + \tau_1 \frac{\partial}{\partial t}\right)\frac{\partial \theta}{\partial x} + H_0^2 \mu_e \left(\frac{\partial^2 u}{\partial x^2} + \frac{\partial^2 v}{\partial x \partial y}\right)$$
$$-\varepsilon_0 H_0^2 \mu_e^2 \frac{\partial^2 u}{\partial t^2} = \rho \frac{\partial^2 u}{\partial t^2} - \rho \Omega^2 u - 2\rho\Omega \frac{\partial v}{\partial t}, \quad (5)$$

$$(\lambda + 2\mu)\frac{\partial^2 v}{\partial y^2} + (\lambda + \mu)\frac{\partial^2 u}{\partial x \partial y} + \mu \frac{\partial^2 v}{\partial x^2} - \gamma_n \frac{\partial N}{\partial y}$$
$$-\gamma_t \left(1 + \tau_1 \frac{\partial}{\partial t}\right)\frac{\partial \theta}{\partial y} + H_0^2 \mu_e \left(\frac{\partial^2 u}{\partial x \partial y} + \frac{\partial^2 v}{\partial y^2}\right)$$
$$-\varepsilon_0 H_0^2 \mu_e^2 \frac{\partial^2 v}{\partial t^2} = \rho \frac{\partial^2 v}{\partial t^2} - \rho \Omega^2 v + 2\rho\Omega \frac{\partial u}{\partial t}, \quad (6)$$

(ii) The plasma (carrier-density) diffusion–recombination equation is [23]

$$D_e \left(\frac{\partial^2 N}{\partial x^2} + \frac{\partial^2 N}{\partial y^2}\right) = \frac{\partial N}{\partial t} + \frac{N}{\tau} - \vartheta \frac{\theta}{\tau}, \quad (7)$$

(iii) The heat equation of thermoelastic semiconductor material is:

$$K\left(\frac{\partial^2 \theta}{\partial x^2} + \frac{\partial^2 \theta}{\partial y^2}\right) = \frac{-E_g}{\tau} N + \rho c_e \left(1 + \tau_0 \frac{\partial}{\partial t}\right)$$
$$+\gamma_t T_0 \left(1 + m\tau_0 \frac{\partial}{\partial t}\right)\left(\frac{\partial^2 u}{\partial x \partial t} + \frac{\partial^2 v}{\partial y \partial t}\right), \quad (8)$$

(iv) The stress-displacement-carrier density-temperature relations are:

$$\sigma_{xx} = (\lambda + 2\mu)\frac{\partial u}{\partial x} + \lambda \frac{\partial v}{\partial y} - \gamma_n N - \gamma_t (1 + \tau_0 \frac{\partial}{\partial t})T$$
$$\sigma_{yy} = (\lambda + 2\mu)\frac{\partial v}{\partial y} + \lambda \frac{\partial u}{\partial x} - \gamma_n N - \gamma_t (1 + \tau_0 \frac{\partial}{\partial t})T$$
$$\sigma_{xy} = \mu(\frac{\partial v}{\partial x} + \frac{\partial u}{\partial y}) \quad (9)$$

where s_0 corresponds to the surface recombination speed, q_0 is a constant parameter, and t_p signifies the characteristic timescale of the pulse heat flux.

It is useful to recast the above equations into a dimensionless form. For this purpose, the following nondimensional variables are introduced:

$$\left(t^*, \tau^*, \tau_0^*, \tau_1^*\right) = \eta c^2 \left(t, \tau, \tau_0, \tau_1\right), \quad (10)$$
$$\left(x^*, y^*, u^*, v^*\right) = \eta c \left(x, y, u, v\right),$$
$$\left(\sigma_{xx}^*, \sigma_{yy}^*, \sigma_{xy}^*\right) = \frac{1}{\mu}\left(\sigma_{xx}, \sigma_{yy}, \sigma_{xy}\right),$$
$$N^* = \frac{N}{n_0}, \ \theta^* = \frac{\theta}{T_0}, \ Q^* = \frac{Q}{n_0 \eta^2 c^2 D_e}, \ \Omega^* = \frac{\Omega}{c},$$

where $\eta = \frac{\rho c_e}{K}$ and $c = \sqrt{\frac{\lambda+2\mu}{\rho}}$.
Using (10) in (5)-(9) after removing the primes, we obtain

$$\frac{\partial^2 u}{\partial x^2} + \gamma_1 \frac{\partial^2 v}{\partial x \partial y} + \gamma_2 \frac{\partial^2 u}{\partial y^2} - \gamma_3 \frac{\partial N}{\partial x}$$
$$-\gamma_4 \left(1 + \tau_1 \frac{\partial}{\partial t}\right)\frac{\partial \theta}{\partial x} + \gamma_5 \left(\frac{\partial^2 u}{\partial x^2} + \frac{\partial^2 v}{\partial x \partial y}\right)$$
$$-\gamma_6 \frac{\partial^2 u}{\partial t^2} = \frac{\partial^2 u}{\partial t^2} - \gamma_7 \Omega^2 u - \gamma_8 \Omega \frac{\partial \mathrm{v}}{\partial \mathrm{t}}, \quad (11)$$

$$\frac{\partial^2 v}{\partial y^2} + \gamma_1 \frac{\partial^2 u}{\partial x \partial y} + \gamma_2 \frac{\partial^2 v}{\partial x^2} - \gamma_3 \frac{\partial N}{\partial y}$$
$$-\gamma_4 \left(1 + \tau_1 \frac{\partial}{\partial t}\right)\frac{\partial \theta}{\partial y} + \gamma_5 \left(\frac{\partial^2 u}{\partial x \partial y} + \frac{\partial^2 v}{\partial y^2}\right)$$
$$-\gamma_6 \frac{\partial^2 v}{\partial t^2} = \frac{\partial^2 v}{\partial t^2} - \gamma_7 \Omega^2 v + \gamma_8 \Omega \frac{\partial \mathrm{u}}{\partial \mathrm{t}}, \quad (12)$$

$$\left(\frac{\partial^2 N}{\partial x^2} + \frac{\partial^2 N}{\partial y^2}\right) = \gamma_9 \frac{\partial N}{\partial t} + \gamma_9 \frac{N}{\tau} - \gamma_{10} \frac{\theta}{\tau}, \quad (13)$$

10.57647/mathsci.2026.2001.02

$$\left(\frac{\partial^2\theta}{\partial x^2}+\frac{\partial^2\theta}{\partial y^2}\right)=\gamma_{11}+\gamma_{12}\left(1+\tau_0\frac{\partial}{\partial t}\right)$$
$$+\gamma_{13}\left(1+m\tau_0\frac{\partial}{\partial t}\right)\left(\frac{\partial^2 u}{\partial x\partial t}+\frac{\partial^2 v}{\partial y\partial t}\right), \quad (14)$$

$$\delta_{xx}=\frac{\partial u}{\partial x}+\gamma_{14}\frac{\partial v}{\partial y}-\gamma_3 N-\gamma_4\left(1+\tau_1\frac{\partial}{\partial t}\right)\theta, \quad (15)$$

$$\delta_{xy}=\left(\frac{\partial u}{\partial y}+\frac{\partial v}{\partial x}\right). \quad (16)$$

where

$$\gamma_1=\frac{(\lambda+\mu)}{(\lambda+2\mu)},\gamma_2=\frac{\mu}{(\lambda+2\mu)},\gamma_3=\frac{\gamma_n n_0}{(\lambda+2\mu)},$$
$$\gamma_4=\frac{\gamma_t T_0}{(\lambda+2\mu)},\gamma_5=\frac{H_0^2\mu_e}{(\lambda+2\mu)},\gamma_6=\frac{\varepsilon_0 H_0^2\mu_e^2c^2}{(\lambda+2\mu)},$$
$$\gamma_7=\frac{\rho\, c_0}{\eta^2c^2\,(\lambda+2\mu)}\ ,\ \gamma_8=\frac{2\rho\, c_0}{\eta\,(\lambda+2\mu)}\ ,$$
$$\gamma_9=\frac{1}{D_e\eta}\ ,\ \gamma_{10}=\frac{\vartheta T_0}{D_e\eta}\ ,\ \gamma_{11}=\frac{-E_g n_0}{KT_0\eta}\ ,$$
$$\gamma_{12}=\frac{\rho c_e}{K\eta}\ ,\ \gamma_{13}=\frac{\gamma_t}{K\eta}\ ,\gamma_{14}=\ \frac{\lambda}{(\lambda+2\mu)}\ .$$

The displacement components may be expressed in terms of scalar and vector potential functions

$$u=\frac{\partial \emptyset}{\partial x}+\frac{\partial \varphi}{\partial y},$$
$$v=\frac{\partial \emptyset}{\partial y}-\frac{\partial \varphi}{\partial x} \quad (17)$$

Using the representation (17) in (11)-(16), we obtain the equations in decoupled form.

$$(1+\gamma_5)\frac{\partial^2\emptyset}{\partial x^2}+(\gamma_1+\gamma_2+\gamma_5)\frac{\partial^2\emptyset}{\partial y^2}-\gamma_3 N \quad (18)$$
$$-\gamma_4\left(1+\tau_1\frac{\partial}{\partial t}\right)\theta-(\gamma_6+1)\frac{\partial^2\emptyset}{\partial t^2}+\gamma_7\Omega^2\emptyset+\gamma_8\Omega\frac{\partial^2\emptyset}{\partial y\partial t}=0$$

$$(\gamma_1-1)\frac{\partial^2\varphi}{\partial y^2}-\gamma_2\frac{\partial^2\varphi}{\partial x^2}+(1-\gamma_6)\frac{\partial^2\varphi}{\partial t^2}$$
$$-\gamma_7\Omega^2\varphi-\gamma_8\Omega\frac{\partial^2\varphi}{\partial y\partial t}=0 \quad (19)$$

$$\left(\frac{\partial^2\theta}{\partial x^2}+\frac{\partial^2\theta}{\partial y^2}\right)=\gamma_{11}N+\gamma_{12}\left(1+\tau_0\frac{\partial}{\partial t}\right)$$
$$+\gamma_{13}\left(1+m\tau_0\frac{\partial}{\partial t}\right)\left(\frac{\partial^2\emptyset}{\partial x^2\partial t}+\frac{\partial^2\varphi}{\partial y^2\partial t}\right) \quad (20)$$

3. Solution Methodology

For a wave propagated in (x-z) plane, the following normal mode analysis method is used [21]:

$$(\emptyset,N,\theta,\psi)(x,y,t)=(\emptyset^*,N^*,\theta^*,\psi^*)(x)e^{(\omega t+iay)} \quad (21)$$

Where ω is the angular frequency of the propagating waves, b denotes the wave number, and i is the imaginary unit.Upon substituting the assumed form (27), the following expression is derived:

$$\left(D^2-m_{17}\right)\psi^*(x)=0 \quad (22)$$

$$(D^2\,m_{11}-m_{12})\emptyset^*(x)-m_{13}\,N^*(x) \quad (23)$$
$$-m_{14}\,\theta^*(x)=0$$

$$\left(D^2-m_{18}\right)\theta^*(x)-m_{19}N^*(x) \quad (24)$$
$$-m_{20}\left(D^2-m_{21}\right)\emptyset^*(x)=0$$

$$\left(D^2-m_{22}\right)N^*(x)+m_{23}\theta^*(x)=0 \quad (25)$$

Where, $m_{11}=1+\gamma_5$, $m_{12}=\gamma_1a^2+\gamma_2a^2+\gamma_5a^2+\gamma_6\omega^2+\omega^2-\gamma_7\Omega^2+\gamma_8\Omega ia\omega$, $m_{13}=\gamma_3$, $m_{14}=\gamma_4(1+\tau_1\omega)$, $m_{15}=-\gamma_2$, $m_{16}=-b^2+\gamma_1b^2+\gamma_6\omega^2-\omega^2+\gamma_7\Omega^2+\gamma_8\Omega ia\omega$, $m_{17}=\frac{m_{16}}{m_{15}}$, $m_{18}=a^2+\gamma_{12}\omega(1+\tau_0\omega)$, $m_{19}=\frac{\gamma_{11}}{\tau}$, $m_{20}=\gamma_{13}\omega(1+m\tau_0\omega)$, $m_{21}=a^2$, $m_{22}=a^2+\gamma_9\omega+\frac{\gamma_9}{\tau}$, $m_{23}=\frac{\gamma_{10}}{\tau}$.
On solving Eqs. (22)- (25), a sixth order homogeneous differential equation is obtained as given by:

$$(D^6-\alpha_{11}D^4+\alpha_{12}D^2-\alpha_{13})(\emptyset^*(x),N^*(x),\theta^*(x))=0 \quad (26)$$

Where, $\alpha_{11}=\frac{K_{12}}{K_{11}}$, $\alpha_{12}=\frac{K_{13}}{K_{11}}$, $\alpha_{13}=\frac{K_{14}}{K_{11}}$, $K_{11}=-m_{11}$, $K_{12}=-m_{21}-m_{14}m_{20}-m_{11}(m_{18}+m_{22})$, $K_{13}=m_{11}m_{18}m_{22}+m_{12}(m_{18}+m_{22})+m_{14}m_{20}(m_{21}+m_{22})+m_{11}m_{19}m_{23}+m_{13}m_{20}m_{23}$, $K_{14}=-m_{12}m_{18}m_{22}-m_{14}m_{20}m_{21}m_{22}-m_{12}m_{19}m_{23}-m_{13}m_{20}m_{21}m_{23}$,
Auxiliary equation for equation (26) is:

$$\lambda^6-a_{11}\lambda^4+a_{12}\lambda^2-a_{13}=0 \quad (27)$$

The solution of equations (26) and (22) - (25) are expressed as:

$$\psi^*(x)=B_1e^{-\delta_1 x} \quad (28)$$
$$\theta^*(x)=A_1e^{-\lambda_1 x}+A_2e^{-\lambda_2 x}+A_3e^{-\lambda_3 x} \quad (29)$$
$$N^*(x)=A_1\,H_{11}e^{-\lambda_1 x}+A_2H_{12}e^{-\lambda_2 x}+A_3H_{13}e^{-\lambda_3 x} \quad (30)$$
$$\emptyset^*(x)=A_1H_{14}e^{-\lambda_1 x}+A_2H_{15}e^{-\lambda_2 x}+A_3H_{16}e^{-\lambda_3 x} \quad (31)$$

Where λ_i^2, $(i=1,2,3)$ are roots of auxiliary equation (27),

$$H_{11}=\frac{-m_{23}}{(\lambda_1^2-m_{22})},H_{12}=\frac{-m_{23}}{(\lambda_2^2-m_{22})},$$
$$H_{13}=\frac{-m_{23}}{\left(\lambda_3^2-m_{22}\right)},H_{14}=\frac{m_{13}\,H_{11}+m_{14}}{m_{11}\lambda_1^2-m_{12}},$$
$$H_{15}=\frac{m_{13}\,H_{11}+m_{14}}{m_{11}\lambda_2^2-m_{12}},H_{15}=\frac{m_{13}\,H_{11}+m_{14}}{m_{11}\lambda_3^2-m_{12}},$$

The definitions for the coefficients $\lambda_1,\lambda_2,\lambda_3,\delta_1$ involved are detailed in Appendix I.

10.57647/mathsci.2026.2001.02

The temperature and displacement components are obtained using equations (20), (21), (23), (27) and (35), as follows:

$$\theta = (A_1 e^{-\lambda_1 x} + A_2 e^{-\lambda_2 x} + A_3 e^{-\lambda_3 x}) e^{\omega t + iay} \quad (32)$$

$$u = (-H_{14} A_1 \lambda_1 e^{-\lambda_1 x} - H_{15} A_2 \lambda_2 e^{-\lambda_2 x} - H_{16} A_3 \lambda_3 e^{-\lambda_3 x} + iaB_1 e^{-\delta_1 x}) e^{\omega t + iay} \quad (33)$$

$$v = \left(ia \left(H_{14} A_1 e^{-\lambda_1 x} + H_{15} A_2 e^{-\lambda_2 x} + H_{16} A_3 \lambda_3 e^{-\lambda_3 x}\right) + B_1 \delta_1 e^{-\delta_1 x}\right) e^{\omega t + iay} \quad (34)$$

Using equations (32), (33) and (34), the stress components can be determined as follows:

$$\sigma_{xx} = \left(A_1 e^{-\lambda_1 x} \left(H_{14}\lambda_1^2 - {}_{14}a^2 H_{14} - \gamma_3 H_{11} - m_{14}\right) + A_2 e^{-\lambda_2 x} \left(H_{15}\lambda_2^2 - \gamma_{14} a^2 H_{15} - \gamma_3 H_{12} - m_{14}\right) + A_3 e^{-\lambda_3 x} \left(H_{16}\lambda_3^2 - \gamma_{14} a^2 H_{16} - \gamma_3 H_{13} - m_{14}\right) + B_1 \delta_1 iae^{-\delta_1 x} (\gamma_{14} - 1)\right) e^{\omega t + iay} \quad (35)$$

$$\sigma_{xy} = (-2A_1 e^{-\lambda_1 x} iaH_{14}\lambda_1 - 2A_2 e^{-\lambda_2 x} iaH_{15}\lambda_2 - 2A_3 e^{-\lambda_3 x} iaH_{16}\lambda_3 - B_1 e^{-\delta_1 x}(a^2 + \delta_1^2)) e^{\omega t + iay} \quad (36)$$

4. Boundary conditions

The problem under consideration involves a thermoelastic half-space subjected to an external heat source. At the boundary surface $x = 0$, the following conditions are imposed:
The boundary condition for normal stress is given by:

$$\sigma_{xx}{}^* = 0 \quad (37)$$

- The boundary condition for shearing stress is defined as follows:

$$\sigma_{xy}^* = 0 \quad (38)$$

- The thermal boundary condition is described as follows:

$$-K \frac{\delta\theta}{\partial x} = \frac{q_0 t^2 e^{\frac{-t}{t_p}}}{16 t_p^2} \quad (39)$$

- The plasma boundary condition is imposed as:

$$D_e \frac{\partial N}{\partial x} - s_0 N = 0 \quad (40)$$

Applying the aforementioned boundary conditions yields a system of three homogeneous equations. This system is solved using Mathematica, allowing the determination of the unknowns A_1, A_2, A_3 and B_1.

$$\left(A_1 \left(H_{14}\lambda_1^2 - \gamma_{14} a^2 H_{14} - \gamma_3 H_{11} - m_{24}\right) + A_2 \left(H_{15}\lambda_2^2 - \gamma_{14} a^2 H_{15} - \gamma_3 H_{12} - m_{24}\right) + A_3 \left(H_{16}\lambda_3^2 - \gamma_{14} a^2 H_{16} - \gamma_3 H_{13} - m_{24}\right) + B_1 \delta_1 ia (\gamma_{14} - 1)) = 0,$$

$$(-2A_1 iaH_{14}\lambda_1 - 2A_2 iaH_{15}\lambda_2 - 2A_3 iaH_{16}\lambda_3 + B_1 \left(-a^2 - \delta_1^2\right)\Big) = 0, A_1 \left(D_e \eta c \left(-H_{11}\lambda_1\right) - s_0 H_{11}\right) + A_2 \left(D_e \eta c \left(-H_{12}\lambda_2\right) - s_0 H_{12}\right) + A_3 \left(D_e \eta c \left(-H_{13}\lambda_3\right) - s_0 H_{13}\right) = 0,$$

$$A_1 K T_0 \lambda_1 + A_2 K T_0 \lambda_2 + A_3 K T_0 \lambda_3 = \frac{q_0 t^2 e^{\frac{-\left(\frac{t}{\eta c}\right)}{t_p}}}{16 \eta^3 c^5 t_p^2}. \quad (41)$$

To determine the constants A_1, A_2, A_3 and B_1, Cramer's method is applied to Eqs. (41).

$$A_1 = \frac{\Delta A_1}{\Delta}, \; A_2 = \frac{\Delta A_2}{\Delta}, \; A_3 = \frac{\Delta A_3}{\Delta}, \; B_1 = \frac{\Delta B_1}{\Delta}.$$

The definitions for the coefficients $\Delta, \Delta A_1, \Delta A_2, \Delta A_3, \Delta B_1$ involved are detailed in Appendix II.

By employing Eqs. (32), (33), (34) and (35) – (36), the displacement, mechanical stress, and temperature fields in the thermoelastic half-space are determined.

5. Validity of the model

When the thermoelastic wave (which is illustrated by rotation is ignored, the thermo-ealastic interactions in thermoelasticity theory in the framework of photo-thermal theory is obtained and the results agree with Ezzat [12]. When the plasma wave (which is illustrated by carrier density $N(x, z, t)$ is ignored, the thermoelasticity theory is obtained and the results agree with Abd-Alla et al. [22].

6. Numerical results and discussion

To complement the theoretical findings derived in the previous sections, we now present a numerical example for specific medium. The numerical analysis is performed using Mathematica software to demonstrate the influence of rotation, magnetic field, electric field, wave number, and time on the various physical fields, the temperature, normal stress, shear stresses, normal displacement, and carrier density due to both types of ramp type heating and photothermal stress, which are illustrated graphically. For numerical computations, the material properties of Silicon as in [15] are taken under consideration, which are as follows:

$$\lambda = 3.64x10^{10} Nm^{-2}, \quad \mu = 5.46x10^{10} Nm^{-2}, \quad k = 10^{10} Nm^{-1}, \quad \rho = 2330 gm^{-3} \quad \gamma = 0.779x10^{-9} N, \quad j = 0.2x10^{-19} m^2, \quad K = 150 Wm^{-1} K^{-1}, \quad K^* = 3Wm^{-1} K^{-1}, \quad c_e = 650 Jkg^{-1} K^{-1}, \quad T_0 = 800K, \quad \tau = 5x10^{-5} s, \quad E_g = 1.11eV, \quad D_e = 2.5x10^{-3} m^2 s^{-1}, \quad d_n = -9x10^{-31} m^3, \quad s_0 = 2ms^{-1}, \quad n_0 = 10^{20} m^{-3}, \quad \alpha_t = 3x10^{-6} K^{-1}, \quad a = 0.25, \quad q_0 = 10.$$

The other constants that are used for numerical calculations are taken as follows:
$\omega = 1.0$, $t = 0.1$, and $b = 1$. The results are plotted at different values of x at $z = 0.5$. To enhance convenience, we have organized the graphs into three distinct

10.57647/mathsci.2026.2001.02

categories. In the first set of groups, Figure 1, Figure 2, Figure 3, Figure 4 and Figure 5 illustrate how the various wave profiles are influenced by the, time t, rotation Ω, magnetic field H_0, electric permittivity ε_0 and laser pulse time t_p utilizing three distinct values of magnetic field, rotation and laser pulse time on the physical quantities.

Figure 1: Clear difference in Variations of the displacement components u, w, temperature θ, stress components σ_{xx}, σ_{xy} and carrier the density N with respect to x−axis for different values of time t. It's observed that the u, w, θ decrease with increasing of axial x, while it increases with increasing of t, as well the stress components σ_{xx}, σ_{xy} increase with increasing with time. Furthermore, it decreases with increasing of time and the carrier density decreases with increasing of time and axial x. Initially, the amplitude experiences an exponential increase, followed by a subsequent increase, ultimately approaching zero at initial distance x.It's noticed that the physical quantities satisfied boundary conditions. These results obey the physical properties of photo-thermoelasticity theory. These results obey the physical properties of photo-thermoelasticity theory. This result is in a good agreement with the results obtained by Othman et al. [17].

Figure 2: demonstrate the influence of characteristic laser Pulse time t_p on the displacement components u, w, temperature θ, stress components σ_{xx}, σ_{xy} and carrier the density N with respect to x−axis. Initially, there is a strong landing in the temperature distribution as distance expands, eventually giving way to a gradual descent. It's observed that the u, w, θ decrease with increasing of axial x, while it increases with increasing of t, as well the stress components σ_{xx}, σ_{xy} increase with increasing with axial x while it decreases with increasing Laser Pulse time. In this figure, both the curves have coincident beginning point with value zero, which leads to satisfy the boundary condition and depletion of magnitude takes place as the distance from the boundary increases. It is noticed that the due to the time effect, the elastic waves on the surface are generated with a positive amplitude, which starts increasing when moving away from the source. It is noticed that the laser pulse time effects significantly affect the physical quantities variation behavior compared to without laser pulse time. It is found that the fact that the effect of laser pulse time effect corresponds to the term signifying positive forces that tend to accelerate the metal particles. This result is in a good agreement with the results obtained by Lotfy et al. [18].

Figure 3: the impact of the angular frequency parameter is shown for three different values of $\omega = 0.5, 1.0, 1.5$. This figure illustrates the main distributions along the horizontal distance x for displacement components u, w, temperature θ, stress components σ_{xx}, σ_{xy} and carrier the density N, within the photo-thermo-mechanical dynamic model. It's observed that the u, θ, N decrease with increasing of axial x, while it increases with increasing of angular frequency ω, as well as the displacement component w decreases with increasing of axial x and angular frequency ω. Furthermore the stress components σ_{xx}, σ_{xy} increase with increasing with axial x, while it decreases with increasing of angular frequency. Hence, the presence of angular frequency enhances the magnitude of $u, w, \theta, \sigma_{xx}, \sigma_{xy}, N$. Additionally, recognizing points of high sensitivity can guide the design of more robust systems that perform consistently across a range of operating conditions. It's noticed that the physical quantities satisfied boundary conditions. It's noticed that the physical quantities satisfied boundary conditions. These results obey the physical properties of photo-thermoelasticity theory. This result is in a good agreement with the results obtained by Kh. Lotfy [19].

Figure 4: portrays the behavior of displacement components u, w, temperature θ, stress components σ_{xx}, σ_{xy} and carrier the density N within a semiconductor medium, shown as a function of distance $x$and impacted by the rotation Ω, analyzed within the realm of hyperbolic two-temperature photothermal wave theory. It's observed that the u, w,θ, N decrease with increasing of axial x, while it increases with increasing of rotation Ω, as well the stress components σ_{xx}, σ_{xy} increase with increasing axial x, while it decreases with increasing of rotation Ω. This behavior is modulated by the rotation strength, indicated by the differing curves for each value of Ω, showing that the rotation exerts a significant control over carrier distribution within the material. It's noticed that the physical quantities satisfied boundary conditions. It is clearly observed that the mechanical waves are highly sensitive towards the characteristic rotation. It is clearly observed that the mechanical waves are highly sensitive towards the characteristic rotation. The normal stress and shear distribution reveals how uncertainties in thermal and mechanical excitation influence stress wave propagation, which is particularly important in high-precision applications. This result is in good agreement with the results obtained by Othman et al. [17].

Figure 5: The given plot illustrates the variation of the physical quantities u, w, θ, σ_{xx}, σ_{xz}, σ_{zz}, N as a function of horizontal distance for different values of electric permittivity ε_0, as indicated in the legend. However, if the electric permittivity increase, there is a clear trend of decreasing magnitude in the physical quantities. This highlights the impactful relationship between the electric permittivity and the resulting amplitude of physical quantities. It's observed that the u decreases with increasing of axial x, while it increases with increasing of electric permittivity ϵ_0, as well the displacement component w, temperature heats θ decreases with increasing of axial x and electric permittivity ϵ_0. Furthermore the stress components σ_{xx}, σ_{xy} increase with increasing with axial x, while σ_{xy} decreases with increasing of electric field ϵ_0, as well σ_{xx} increases with increasing of ϵ_0. Also, the carrier the density N decreasing with increasing of axial x and ϵ_0. The u, w, θ, σ_{xx}, σ_{xz}, σ_{zz}, N reveal how uncertainties in thermal and mechanical excitation influence stress

wave propagation, which is particularly important in high-precision applications. It's noticed that the physical quantities satisfied boundary conditions. This result is in a good agreement with the results obtained by Al-Hazaemh et al. [23].

Figure 6: illustrates the physical quantities u, w, T, σ_{xx}, σ_{xz}, σ_{zz}, N as a function of horizontal distance for different values of magnetic field H_0. It's observed that the u, w,θ, N decrease with increasing of axial x and magnetic field H_0. Furthermore the stress components σ_{xx} increases with increasing with axial x, while it decreases with increasing of magnetic field H_0, σ_{xy} increases with increasing with axial x and magnetic field H_0. It's noticed that the physical quantities satisfied boundary conditions. The u, w, T, σ_{xx}, σ_{xz}, σ_{zz}, N reveal how uncertainties in thermal and mechanical excitation influence stress wave propagation, which is particularly important in high-precision applications. This result is in a good agreement with the results obtained by Abd-Alla and Abo-Dahab [20].

Figure 7: displays the physical quantities u, w, T, σ_{xx}, σ_{xz}, σ_{zz}, N, across a semiconductor medium as a function of distance (x), influenced by wave number (a). It's observed that the u,θ, N decrease with increasing of axial x and wave number a, as well the displacement component w increases with increasing of axial x , while it decreases with increasing of wave number a. Furthermore the stress components σ_{xx}, σ_{xy} increase with increasing with axial x as well σ_{xx}, σ_{xy} increases with increasing of a. The variation in the profiles with different wave number highlights the wave number impact on the the physical quantities within the material. This graph serves to elucidate the material's thermodynamic response under the simultaneous action of wave number within the theoretical framework described. It's noticed that the physical quantities satisfied boundary conditions. The normal stress and shear stress distribution reveals how uncertainties in thermal and mechanical excitation influence stress wave propagation, which is particularly important in high-precision applications. This result is in a good agreement with the results obtained by Lotfy and El-Bary [15].

7. Conclusion

In this manuscript, we explored the dynamics of rotation, the interplay between thermal waves, plasma, and elastic waves within a homogeneous medium of a two-dimensional deformation semiconductor material, employing electro-magneto-photo-thermoelasticity theory. By applying both the normal mode analysis and Lame's potential, we derived analytical formulas for various physical quantities. To understand the full scope of the parameters' impact, a comprehensive study involving both graphical and theoretical analysis was undertaken. The findings from these investigations can be distilled into several key points:

1. All the physical quantities display a consistent qualitative pattern for different values of time, laser pulse time, angular frequency, electric permittivity, magnetic field, rotation and wave number. It is observed that, as time progresses, there is a noticeable increase in the magnitude of all the field variables. This indicates that the thermal and mechanical responses of the medium evolve over parameters, amplifying the effects of parameter.

2. All physical variables temperature, displacement components, stresses components and carrier density grow over time, indicating progressive thermal and mechanical responses under applied loads.

3. The validity of the thermoelasticity theory is reinforced by the observation that all physical variables attain nonzero values only within a finite region of the medium. This localization of thermal and mechanical responses, as illustrated in the graphical results.

4. **Magnetic Field Effects:** Magnetic fields significantly influence all measured physical quantities. Our findings indicate that these factors enhance the profiles of physical quantities.

5. **Electric permittivity Effects:** The presence of electric permittivity markedly influences all investigated physical quantities. It notably decreases the stress magnitude while augmenting the values of temperature, displacement components, stress components and carrier density, illustrating the pivotal role of electric permittivity in modulating the system's characteristics.

6. **Spatial Distribution:** All physical variables manifest non-zero values exclusively within a confined spatial region, as illustrated in the figures. Moreover, as distance increases, all physical quantities distributions converge towards zero, achieving equilibrium and adhering to the boundary conditions. This spatial behavior underscores the localized nature of the phenomena and the system's approach to equilibrium over distance.

7. The influence of rotation, electro-magnetic field and laser pulse timeintroduced play a significant role in the temperature, displacement components, stress components, and carrier density, according to numerical data and analysis.

8. Major changes have been visualized between the plotted curves related to all physical quantities due to the laser pulse time, rotation and electromagnetic field in a wide range of the distance which reflects that laser pulse time, rotation and electro-magnetic field dominates every physical quantities a very diminutive range of distance.

In conclusion, our study provides comprehensive insights into the complex interactions between temperature, rotation, electric field and magnetic fields in photothermoelastic semiconductor materials. The significant

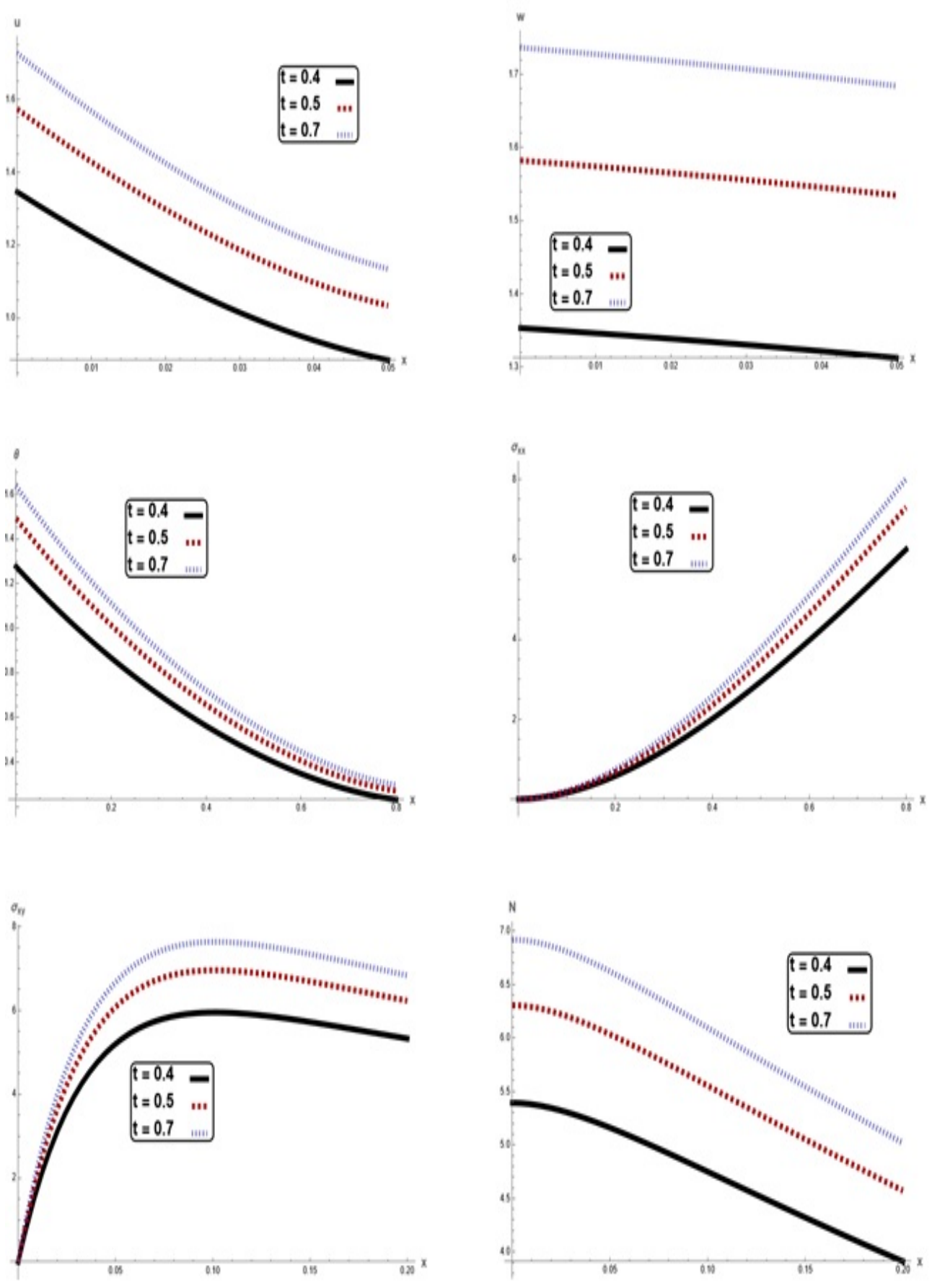

Figure 1. Variation of physical quantities u, w, θ, σ_{xx}, σ_{xy}, N for different values of time t against.

10.57647/mathsci.2026.2001.02

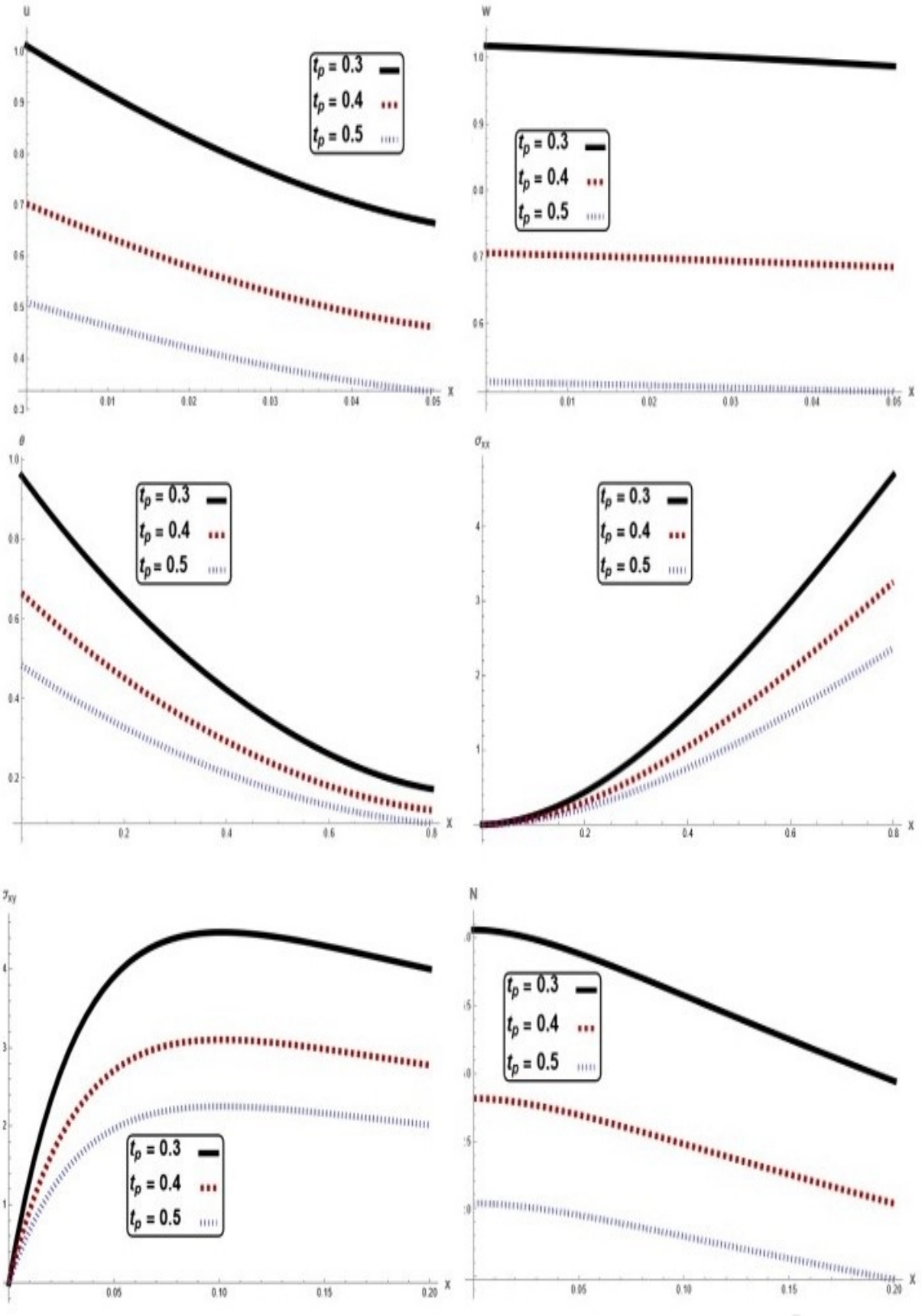

Figure 2. Variation of physical quantities u, w, θ, σ_{xx}, σ_{xy}, N for different values of laser Pulse time t_p against $x-$ axis

10.57647/mathsci.2026.2001.02

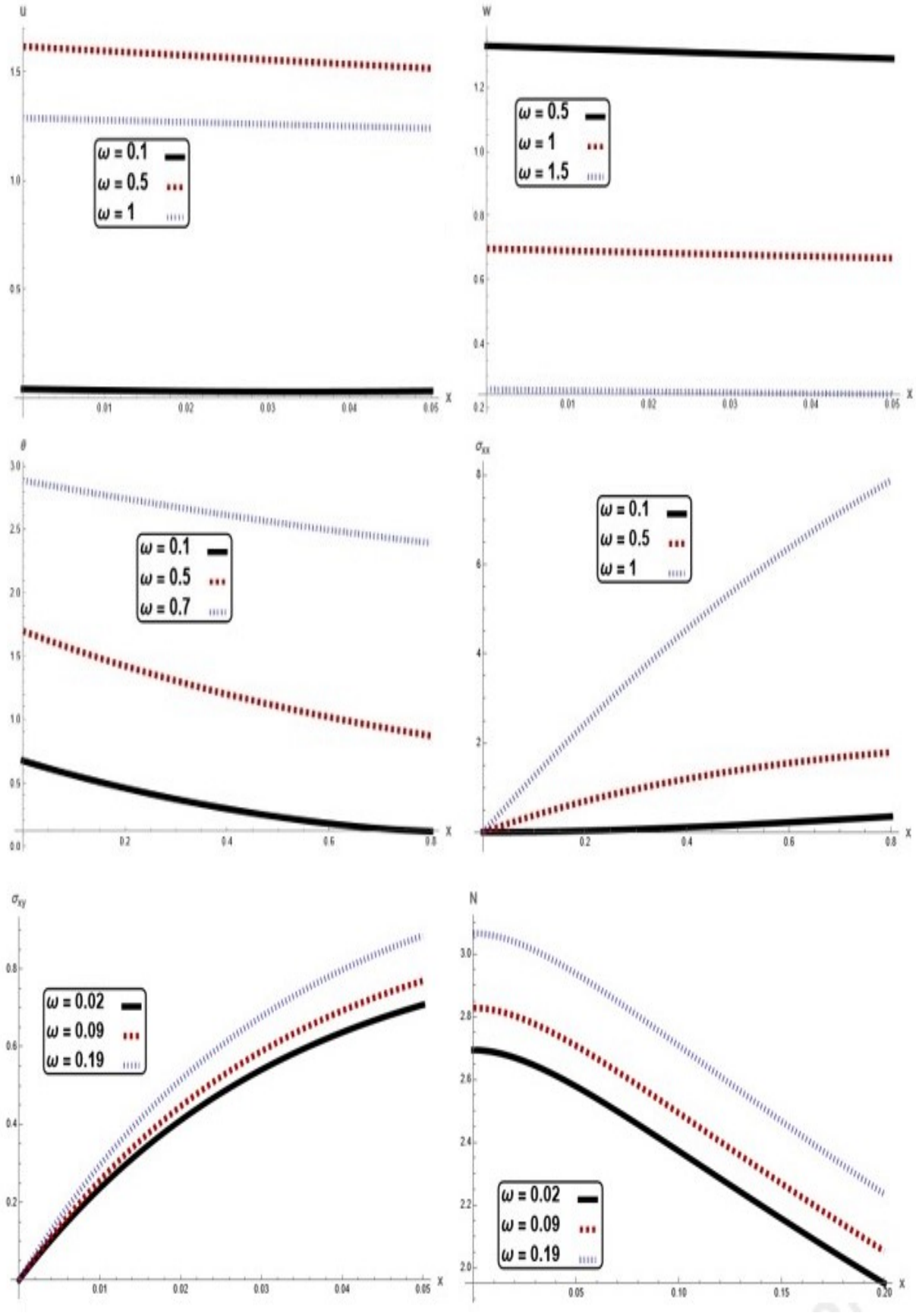

Figure 3. Variation of physical quantities u, w, θ, σ_{xx}, σ_{xy}, N for different values of angular frequency ω against $x-$ axis

10.57647/mathsci.2026.2001.02

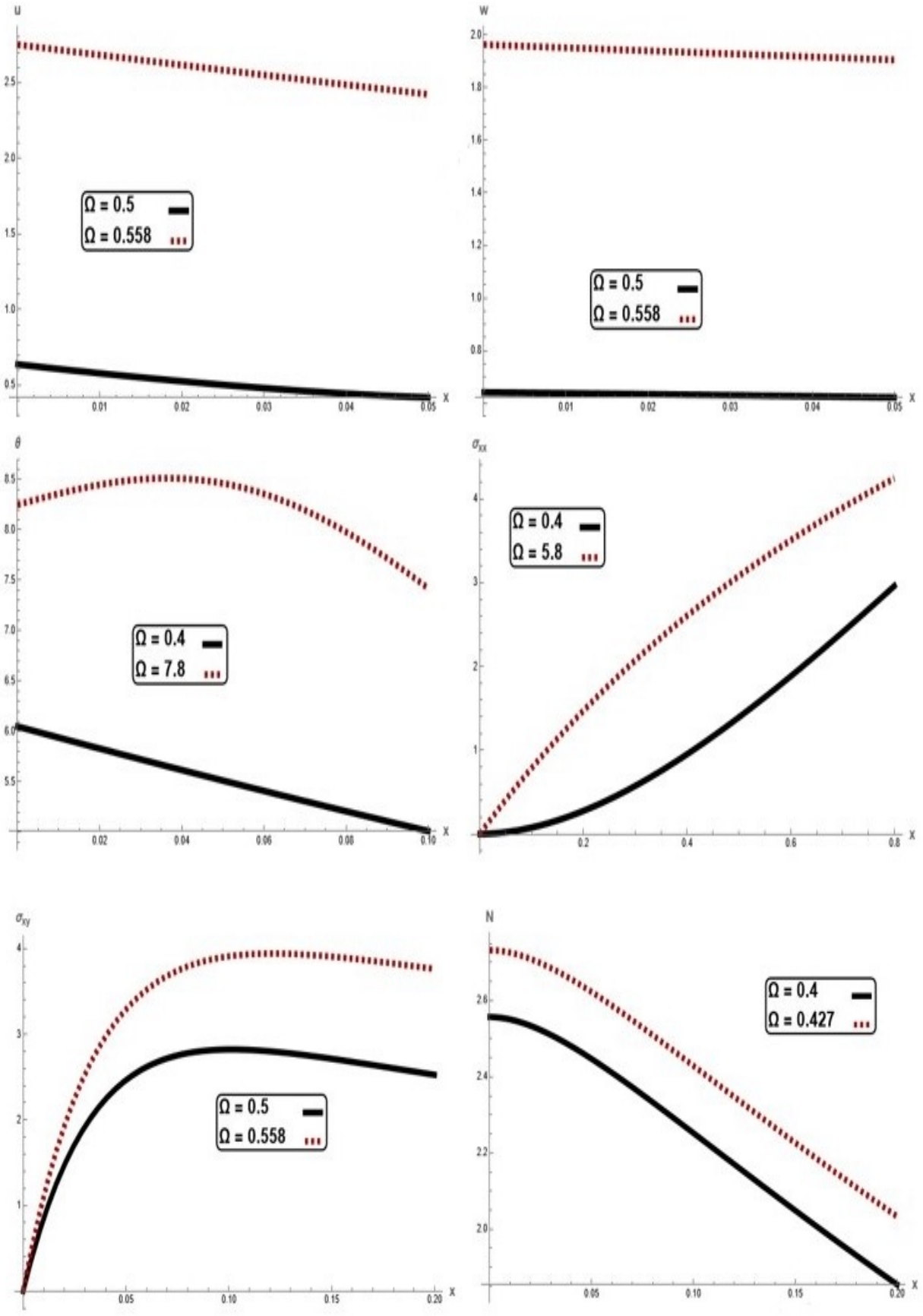

Figure 4. Variation of physical quantities u, w, θ, σ_{xx}, σ_{xy}, N for different values of rotation Ω against x−axis

10.57647/mathsci.2026.2001.02

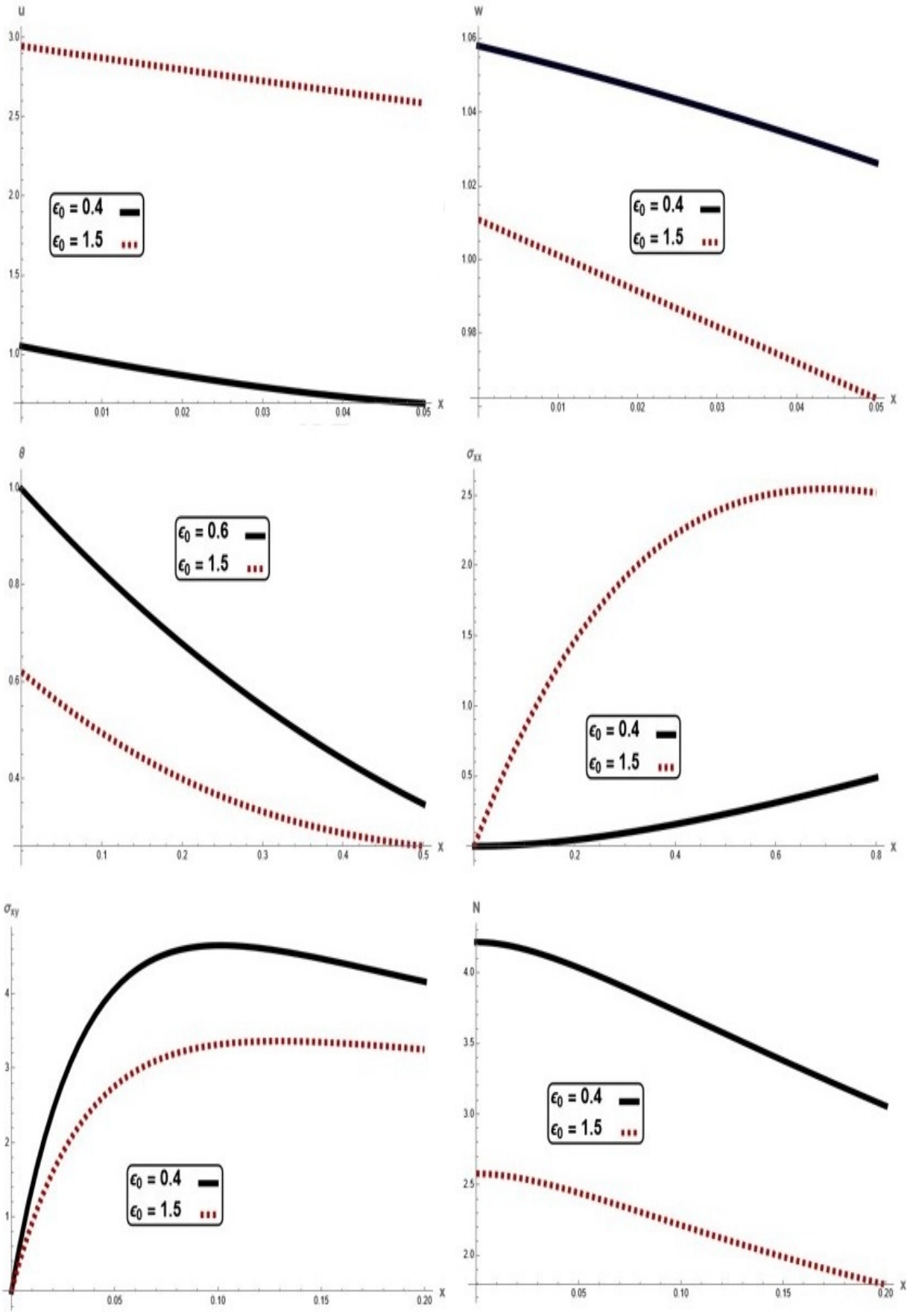

Figure 5. Variation of physical quantities u, w, θ, σ_{xx}, σ_{xy}, N for different values of electric field ε_0 against x−axis

10.57647/mathsci.2026.2001.02

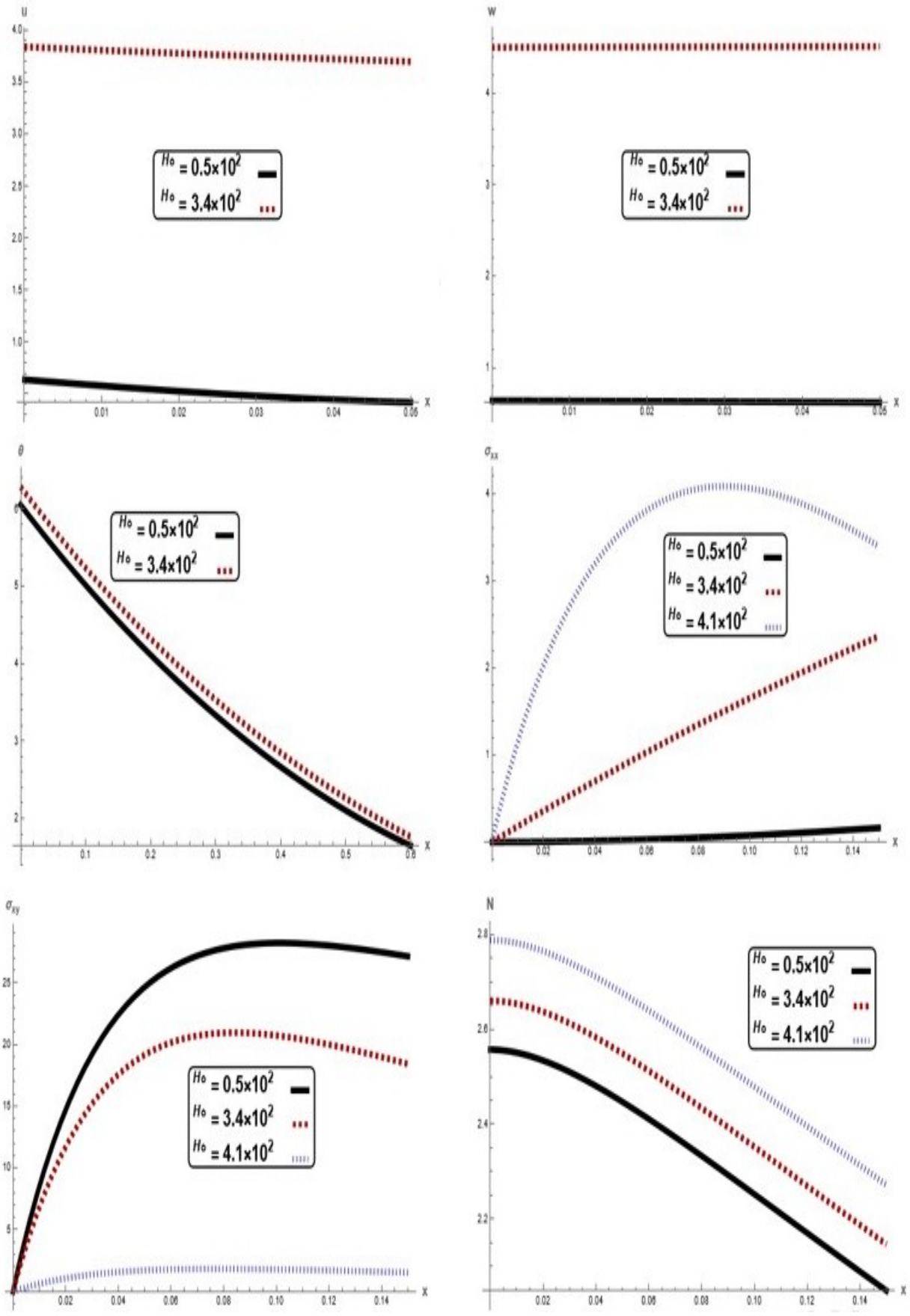

Figure 6. Variation of physical quantities u, w, θ, σ_{xx}, σ_{xy}, N for different values of magnetic field H_0 against x−axis

10.57647/mathsci.2026.2001.02

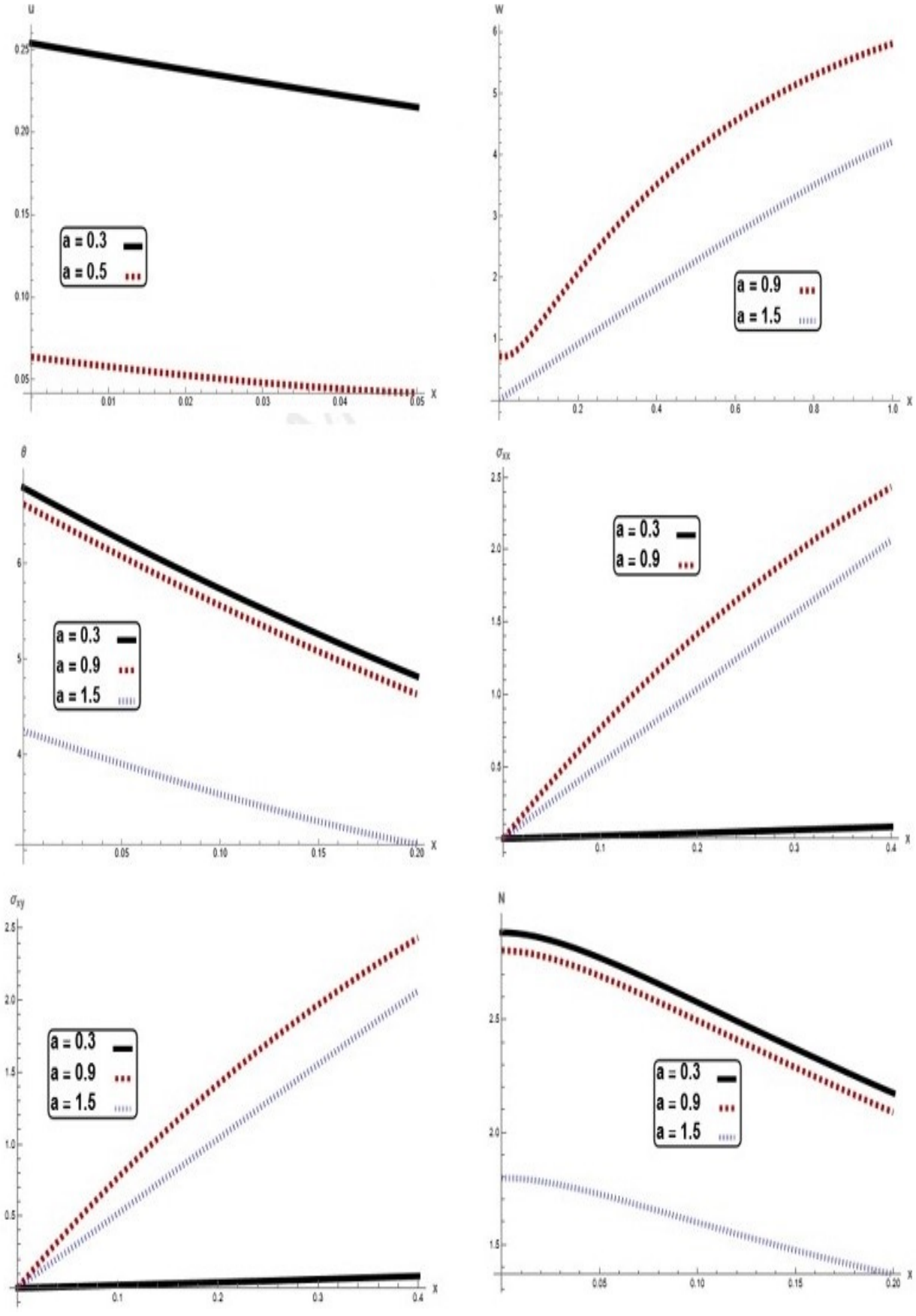

Figure 7. Variation of physical quantities u, w, θ, σ_{xx}, σ_{xy}, N for different values of wave number a against x−axis

10.57647/mathsci.2026.2001.02

influences of parameter, the pivotal impact of temperature, and the spatial distribution of physical variables offer valuable perspectives for understanding the behavior of such systems under various conditions.

8. Future works

We are interested in

- Studing the nonlinear behavior (bending, vibrations,..) of nanocomposite structures emplying some numerical methods such as the differential quadrature method and finite element method.
- The periodic solution of nonlinear equations of a finite deformation of elastic structures will be also considered in the future work.
- Coupled thermo-hydro-mechanical photoelastic wave propagation in poro-semiconductors under gravity and electromagnetic fields.

Funding

This work was supported by the Deanships of Scientific Research, Vice Presidency for Graduate Studies and Scientific Research, King Faisal University, Saudi Arabia [Grant No. KFU260147].

Authors contributions

All the authors have participated sufficiently in the intellectual content, conception and design of this work or the analysis and interpretation of the data (when applicable), as well as the writing of the manuscript.

Availability of data and materials

The data that support the findings of this study are available from the corresponding author, upon reasonable request.

Conflict of interests

The author declare that they have no known competing financial interests or personal relationships that could have appeared to influence the work reported in this paper.

References

1. Biot M. Thermoelasticity and irreversible thermodynamics. Journal of Applied Physics 1956; 27:240–53
2. Lord H and Shulman Y. Generalized dynamical theory of thermoelasticity. Journal of the Mechanics and Physics of Solids 1967; 15:299–309
3. Green A and Lindsay K. Thermoelasticity. Journal of Elasticity 1972; 2:1–7
4. Ignaczak J. Uniqueness in generalized thermoelasticity. Journal of Thermal Stresses 1979; 2:171–5
5. Ignaczak J. A note on uniqueness in thermoelasticity with one relaxation time. Journal of Thermal Stresses 1982; 5:257–63
6. Al-Hazaemh A, Abd-Alla A, and Abbas S. Photothermal interactions in micropolar generalized thermoelastic medium subjected to electromagnetic field. Scientific Reports 2025; 15
7. Raddadi M, Mahdy A, El-Bary A, Lotfy K, and Allan M. A rotating magneto-photothermoelastic effect with moisture diffusivity of nonlocal semiconductor medium. The Journal of Strain Analysis for Engineering Design 2024; 59:309–22
8. Abo-Dahab S, Salah D, Gafel H, Abd-Alla A, and Abdelhafez M. Electromagnetic and heated pulse laser on wave propagation during electrons and holes excitation processes in a rotator semiconductor medium. Scientific Reports 2025; 15
9. Othman M and Singh S. Photo-thermoelastic interaction in a semiconductor medium with temperature-dependent properties. Journal of Thermal Stresses 2005; 28:841–64
10. Sherief M, El-Sayed A, and Abd-Alla A. Generalized magneto-thermoelastic interactions in a rotating non-homogeneous solid. Acta Mechanica 2003; 162:1–17
11. Tzou D. Macro- to micro-scale heat conduction including non-Fourier effects. Journal of Heat Transfer 1995; 117:8–16
12. Ezzat M. Thermoelastic interactions induced by a pulsed laser beam in a semiconductor medium. Applied Mathematics and Computation 2005; 165:431–44
13. El-Bary A, Raddadi M, and Lotfy K. Magneto-thermoelastic waves in a semiconductor medium with temperature-dependent conductivity. International Journal of Applied Mechanics 2021; 13:2150021
14. Lord H and Shulman Y. A generalized dynamical theory of thermoelasticity. Journal of the Mechanics and Physics of Solids 1967; 15:299–309
15. Lotfy K and El-Bary A. Photothermal excitation in semiconductor media under fractional-order thermoelastic theory. Thermal Science 2020; 24:1561–70
16. Tiwari R, Saeed A, Kumar R, Kumar A, and Singhal A. Memory response on generalized thermoelastic medium in context of dual phase lag thermoelasticity with non-local effect. Journal of Archives of Mechanics 2022; 74:69–88

17. Othman M, Hasona W, and Abd-Elaziz E. Effect of rotation on micropolar generalized thermoelasticity with two-temperatures using a dual-phase lag model. Canadian Journal of Physics 2014; 92:149–58
18. Abd-Alla A and Al-Qahtani M. Electro-magneto-thermoelastic wave propagation in a rotating anisotropic semiconductor. International Journal of Engineering Science 2011; 49:276–85
19. Lotfy K. The elastic wave motions for a photothermal medium of a dual-phase-lag model with an internal heat source and gravitational field. Canadian Journal of Physics 2016; 94:400–9
20. Abd-Alla A and Abo-Dahab S. Effect of rotation and initial stress on an infinite generalized magneto-thermoelastic diffusion body with a spherical cavity. Journal of Thermal Stresses 2012; 35:892–912
21. Jangra A, Sheok P, and Deswal S. Wave propagation in a nonlocal microstretch saturated porothermoelastic medium under moore-gibson-thompson heat conduction model. The Journal of Strain Analysis for Engineering Design 2025; 60:88–105
22. Abd-Alla A, Abo-Dahab S, and Alsharif A. Thermal shock behaviour on generalized thermoelastic medium under initial stress with rotation. Mechanics of Solids 2024; 59:2861–75
23. Awwad E, Abouelregal A, Atta D, and Sedighi H. Photo-thermoelastic behavior of a functionally graded semiconductor medium excited by thermal laser pulses. Physica Scripta 2022; 97
24. Marin M, Agarwal R, and Abbas I. Effect of intrinsic rotations, microstructural expansion and contractions in initial boundary value problem of thermoelastic bodies. Boundary Value Problems 2014; 2014:129
25. Abouelregal A, Marin M, and Öchsner A. The influence of a non-local Moore-Gibson-Thompson heat transfer model on an underlying thermoelastic material under the model of memory-dependent derivatives. Continuum Mechanics and Thermodynamics 2023; 35:545–62
26. Vlase S, Negrean I, Marin M, and Scutaru M. Energy of accelerations used to obtain the motion equations of a three-dimensional finite element. Symmetry 2020; 12:321
27. Alshehri H, Lotfy K, Mahdy AM, and El-Bary A. Double-temperature theory and acoustic pressure impact on magneto-thermoelastic interactions subjected to laser heating. Journal of Vibration Engineering and Technologies 2025; 13:455–67
28. Nassar T, Mahdy AM, and Lotfy K. Thermal Laser Pulse Effect on Optoelectronic Semiconductor Medium with Temperature Dependence and Moisture Diffusivity. Journal of Vibration Engineering and Technologies 2025; 13:485–500
29. Ailawalia P, Kamel A, Mahdy AM, Elidy E, and Lotfy K. Thermal shock analysis in a semiconducting medium using a modified Green–Lindsay thermoelastic model. Mechanics of Solids 2025; 60:1–15
30. Mahdy AM. Stability, existence, and uniqueness for solving fractional glioblastoma multiforme using a Caputo-Fabrizio derivative. Mathematical Methods in the Applied Sciences 2025; 48:7360–77
31. Mahdy M.A. Abdou DSM. Computational methods and dynamical analysis for studying dimensional functional equations of mixed integro-differential type. Boundary Value Problems 2025; 2025:108–15
32. Mahdy AM, Abdou M, and Mohamed DS. Numerical solution, convergence and stability of error to solve quadratic mixed integral equation. Journal of Applied Mathematics and Computing 2024; 70:5887–916
33. Lotfy K, Mahdy A, El-Bary AA, and Elidy E. Magneto-Photo-Thermoelastic Excitation Rotating Semiconductor Medium Based on Moisture Diffusivity. CMES – Computer Modeling in Engineering and Sciences 2024; 141:107–26

Appendix I

$$
\begin{aligned}
\lambda_1 &= \sqrt{\left(\frac{\alpha 11}{3} + \frac{2^{1/3}\alpha 11^2}{3\left(2\alpha 11^3 - 9\alpha 11\alpha 12 + 27\alpha 13 + 3\sqrt{3}\sqrt{-\alpha 11^2\alpha 12^2 + 4\alpha 12^3 + 4\alpha 11^3\alpha 13 - 18\alpha 11\alpha 12\alpha 13 + 27\alpha 13^2}\right)^{1/3}}\right.} \\
&\quad - \frac{2^{1/3}\alpha 12}{\left(2\alpha 11^3 - 9\alpha 11\alpha 12 + 27\alpha 13 + 3\sqrt{3}\sqrt{-\alpha 11^2\alpha 12^2 + 4\alpha 12^3 + 4\alpha 11^3\alpha 13 - 18\alpha 11\alpha 12\alpha 13 + 27\alpha 13^2}\right)^{1/3}} \\
&\quad \left. + \frac{\left(2\alpha 11^3 - 9\alpha 11\alpha 12 + 27\alpha 13 + 3\sqrt{3}\sqrt{-\alpha 11^2\alpha 12^2 + 4\alpha 12^3 + 4\alpha 11^3\alpha 13 - 18\alpha 11\alpha 12\alpha 13 + 27\alpha 13^2}\right)^{1/3}}{32^{1/3}}\right) \\
\lambda_2 &= \sqrt{\left(\frac{\alpha 11}{3} - \frac{\lambda 11^2}{32^{2/3}\left(2\alpha 11^3 - 9\alpha 11\alpha 12 + 27\alpha 13 + 3\sqrt{3}\sqrt{-\alpha 11^2\alpha 12^2 + 4\alpha 12^3 + 4\alpha 11^3\alpha 13 - 18\alpha 11\alpha 12\alpha 13 + 27\alpha 13^2}\right)^{1/3}}\right.} \\
&\quad + \frac{\alpha 11^2}{2^{2/3}\sqrt{3}\left(2\alpha 11^3 - 9\alpha 11\alpha 12 + 27\alpha 13 + 3\sqrt{3}\sqrt{-\alpha 11^2\alpha 12^2 + 4\alpha 12^3 + 4\alpha 11^3\alpha 13 - 18\alpha 11\alpha 12\alpha 13 + 27\alpha 13^2}\right)^{1/3}} \\
&\quad + \frac{\alpha 12}{2^{2/3}\left(2\alpha 11^3 - 9\alpha 11\alpha 12 + 27\alpha 13 + 3\sqrt{3}\sqrt{-\alpha 11^2\alpha 12^2 + 4\alpha 12^3 + 4\alpha 11^3\alpha 13 - 18\alpha 11\alpha 12\alpha 13 + 27\alpha 13^2}\right)^{1/3}} \\
&\quad - \frac{\sqrt{3}\alpha 12}{2^{2/3}\left(2\alpha 11^3 - 9\alpha 11\alpha 12 + 27\alpha 13 + 3\sqrt{3}\sqrt{-\alpha 11^2\alpha 12^2 + 4\alpha 12^3 + 4\alpha 11^3\alpha 13 - 18\alpha 11\alpha 12\alpha 13 + 27\alpha 13^2}\right)^{1/3}} \\
&\quad - \frac{\left(2\alpha 11^3 - 9\alpha 11\alpha 12 + 27\alpha 13 + 3\sqrt{3}\sqrt{-\alpha 11^2\alpha 12^2 + 4\alpha 12^3 + 4\alpha 11^3\alpha 13 - 18\alpha 11\alpha 12\alpha 13 + 27\alpha 13^2}\right)^{1/3}}{62^{1/3}} \\
&\quad \left. - \frac{\mathrm{i}\left(2\alpha 11^3 - 9\alpha 11\alpha 12 + 27\alpha 13 + 3\sqrt{3}\sqrt{-\alpha 11^2\alpha 12^2 + 4\alpha 12^3 + 4\alpha 11^3\alpha 13 - 18\alpha 11\alpha 12\alpha 13 + 27\alpha 13^2}\right)^{1/3}}{22^{1/3}\sqrt{3}}\right) \\
\lambda_3 &= \sqrt{\left(\frac{\alpha 11}{3} - \frac{\alpha 11^2}{32^{2/3}\left(2\alpha 11^3 - 9\alpha 11\alpha 12 + 27\alpha 13 + 3\sqrt{3}\sqrt{-\alpha 11^2\alpha 12^2 + 4\alpha 12^3 + 4\alpha 11^3\alpha 13 - 18\alpha 11\alpha 12\alpha 13 + 27\alpha 13^2}\right)^{1/3}}\right.} \\
&\quad - \frac{\mathrm{i}\alpha 11^2}{2^{2/3}\sqrt{3}\left(2\alpha 11^3 - 9\alpha 11\alpha 12 + 27\alpha 13 + 3\sqrt{3}\sqrt{-\alpha 11^2\alpha 12^2 + 4\alpha 12^3 + 4\alpha 11^3\alpha 13 - 18\alpha 11\alpha 12\alpha 13 + 27\alpha 13^2}\right)^{1/3}} \\
&\quad + \frac{\alpha 12}{2^{2/3}\left(2\alpha 11^3 - 9\alpha 11\alpha 12 + 27\alpha 13 + 3\sqrt{3}\sqrt{-\alpha 11^2\alpha 12^2 + 4\alpha 12^3 + 4\alpha 11^3\alpha 13 - 18\alpha 11\alpha 12\alpha 13 + 27\alpha 13^2}\right)^{1/3}} \\
&\quad + \frac{\mathrm{i}\sqrt{3}\alpha 12}{2^{2/3}\left(2\alpha 11^3 - 9\alpha 11\alpha 12 + 27\alpha 13 + 3\sqrt{3}\sqrt{-\alpha 11^2\alpha 12^2 + 4\alpha 12^3 + 4\alpha 11^3\alpha 13 - 18\alpha 11\alpha 12\alpha 13 + 27\alpha 13^2}\right)^{1/3}} \\
&\quad - \frac{\left(2\alpha 11^3 - 9\alpha 11\alpha 12 + 27\alpha 13 + 3\sqrt{3}\sqrt{-\alpha 11^2\alpha 12^2 + 4\alpha 12^3 + 4\alpha 11^3\alpha 13 - 18\alpha 11\alpha 12\alpha 13 + 27\alpha 13^2}\right)^{1/3}}{62^{1/3}} \\
&\quad \left. + \frac{\mathrm{i}\left(2\alpha 11^3 - 9\alpha 11\alpha 12 + 27\alpha 13 + 3\sqrt{3}\sqrt{-\alpha 11^2\alpha 12^2 + 4\alpha 12^3 + 4\alpha 11^3\alpha 13 - 18\alpha 11\alpha 12\alpha 13 + 27\alpha 13^2}\right)^{1/3}}{22^{1/3}\sqrt{3}}\right), \\
\delta_1 &= \sqrt{m_{17}}.
\end{aligned}
$$

10.57647/mathsci.2026.2001.02

Appendix II

$$\begin{aligned}\Delta &= KT0(-2a^2(-1+\alpha 14)\delta 1(H11(H15-H16)(s0+cDe\eta\lambda 1)\lambda 23 - H12(H14-H16)\lambda 1(s0\\ &+cDe\eta\lambda 2)\lambda 3 + H13(H14-H15)\lambda 1\lambda 2(s0+cDe\eta\lambda 3)) + (-a^2-\delta 1^2)(H12(m24+a^2H14\alpha 14+H11\gamma 3\\ &-H14\lambda 1^2)(s0+cDe\eta\lambda 2)\lambda 3 - H11(s0+cDe\eta\lambda 1)(m24+a^2H15\alpha 14+H12\gamma 3-H15\lambda 2^2)\lambda 3\\ &-H13(m24+a^2H14\alpha 14+H11\gamma 3-H14\lambda 1^2)\lambda 2(s0+cDe\eta\lambda 3)+H13\lambda 1(m24+a^2H15\alpha 14\\ &+H12\gamma 3-H15\lambda 2^2)(s0+cDe\eta\lambda 3)+H11(s0+cDe\eta\lambda 1)\lambda 2(m24+a^2H16\alpha 14+H13\gamma 3-H16\lambda 3^2)\\ &-H12\lambda 1(s0+cDe\eta\lambda 2)(m24+a^2H16\alpha 14+H13\gamma 3-H16\lambda 3^2)))\end{aligned}$$

$$\begin{aligned}\Delta A_1 &= -\frac{1}{16c^5tp^2\eta^3}e^{-\frac{t}{tp\eta c}}q0t^2(H13(-2a^2H15(-1+14)\delta 1\lambda 2+(a^2+\delta 1^2)(m24+a^2H15\alpha 14+H12\gamma 3\\ &-H15\lambda 2^2))(s0+cDe\eta\lambda 3)-H12(s0+cDe\eta\lambda 2)(-2a^2H16(-1+\alpha 14)\delta 1\lambda 3+(a^2+\delta 1^2)(m24\\ &+a^2H16\alpha 14+H13\gamma 3-H16\lambda 3^2)))\end{aligned}$$

$$\begin{aligned}\Delta A_2 &= \frac{1}{16c^5tp^2\eta^3}e^{-\frac{t}{tp\eta c}}q0t^2(H13(-2a^2H14(-1+\alpha 14)\delta 11+(a^2+\delta 1^2)(m24+a^2H14\alpha 14\\ &+H11\gamma 3-H14\lambda 1^2))(s0+cDe\eta\lambda 3)-H11(s0+cDe\eta\lambda 1)(-2a^2H16(-1+\alpha 14)\delta 1\lambda 3\\ &+(a^2+\delta 1^2)(m24+a^2H16\alpha 14+H13\gamma 3-H16\lambda 3^2)))\end{aligned}$$

$$\begin{aligned}\Delta A_3 &= -\frac{1}{16c^5tp^2\eta^3}e^{-\frac{t}{tp\eta c}}q0t^2(H12(-2a^2H14(-1+\alpha 14)\delta 1\lambda 1+(a^2+\delta 1^2)(m24+a^2H14\alpha 14\\ &+H11\gamma 3-H14\lambda 1^2))(s0+cDe\eta\lambda 2)-H11(s0+cDe\eta\lambda 1)(-2a^2H15(-1+\alpha 14)\delta 1\lambda 2\\ &+(a^2+\delta 1^2)(m24+a^2H15\alpha 14+H12\gamma 3-H15\lambda 2^2)))\end{aligned}$$

$$\begin{aligned}\Delta B_1 &= \frac{1}{8c^5tp^2\eta^3}iae^{-\frac{t}{tp\eta c}}q0t^2(H11(s0+cDe\eta\lambda 1)(H15m24\lambda 2-H16m24\lambda 3+H15H16(\lambda 2-\lambda 3)\\ &(a^2\alpha 14+\lambda 2\lambda 3))+H13(H14(m24\lambda 1+H15(\lambda 1-\lambda 2)(a^2\alpha 14+\lambda 1\lambda 2))(s0+cDe\eta\lambda 3)\\ &-H15\lambda 2(cDeH11\gamma 3\eta(-\lambda 1+\lambda 3)+m24(s0+cDe\eta\lambda 3)))+H12(H16(cDeH11\gamma 3\eta\\ &(-\lambda 1+\lambda 2)+m24(s0+cDe\eta\lambda 2))\lambda 3-H14(m24\lambda 1(s0+cDe\eta\lambda 2)\\ &+a^2H16\alpha 14(s0+cDe\eta\lambda 2)(\lambda 1-\lambda 3)+H16s0\lambda 1(\lambda 1-\lambda 3)\lambda 3\\ &+cDe\eta\lambda 1(H13\gamma 3(\lambda 2-\lambda 3)+H16\lambda 2(\lambda 1-\lambda 3)\lambda 3))))\end{aligned}$$

10.57647/mathsci.2026.2001.02